Hindawi Publishing Corporation
Journal of Robotics
Volume 2010, Article ID 609391, 7 pages
doi:10.1155/2010/609391

Research Article

The Kinematics Analysis of a Novel 3-DOF Cable-Driven Wind Tunnel Mechanism

Yao Yu[1] and Wu Hongtao[2]

[1] *College of Aerospace Engineering, NUAA, 29 Yudao Stree, Nanjing, 210016, China*
[2] *College of Mechanical and Electrical Engineering, NUAA, 29 Yudao Street, Nanjing, 210016, China*

Correspondence should be addressed to Yao Yu, yy503@126.com

Received 11 March 2010; Accepted 29 April 2010

Academic Editor: Bijan Shirinzadeh

The kinematics analysis method of a novel 3-DOF wind tunnel mechanism based on cable-driven parallel mechanism is provided. Rodrigues' parameters are applied to express the transformation matrix of the wire-driven mechanism in the paper. The analytical forward kinematics model is described as three quadratic equations using three Rodridgues' parameters based on the fundamental theory of parallel mechanism. Elimination method is used to remove two of the variables, so that an eighth-order polynomial with one variable is derived. From the equation, the eight sets of Rodridgues' parameters and corresponding Euler angles for the forward kinematical problem can be obtained. In the end, numerical example of both forward and inverse kinematics is included to demonstrate the presented forward-kinematics solution method. The numerical results show that the method for the position analysis of this mechanism is effective.

1. Introduction

Parallel manipulators have separate serial kinematic chains that are linked to the ground and the moving platform at the same time. They have some potential advantages over serial robot manipulators such as accuracy, greater load capacity, higher velocities, and accelerations. Parallel manipulators have been developed for applications in many fields [1–4].

In the past few decades, parallel manipulators using cable transmission have been enthusiastically studied in a number of areas. In a cable suspended parallel robot, the moving platform is suspended and manipulated by the attached cables that are connected to the base; for example cable-suspended robots are Robocrane [5, 6], ultra-high-speed cable robot [7], dexterous hands [8, 9], parallel cable-suspended manipulators [10, 11], teleoperating robots [12], and robots for biological use [13]. The major advantage of using tendon transmission lies in that actuators can be installed on the remote base such that a lightweight and compact design can be realized.

In recent years, many researchers paid great attention to the use of cable-driven mechanism in wind tunnel test due to its fewer interference on the streamline flow. Some successful achievements have been made in the Suspension ACtive pour Soufflerie (**SACSO**) project about the cable-driven parallel suspension system in low-speed wind tunnels with 8 cables [14], another application is WDPSS-8 developed by Huaqiao university for use in wind tunnel test [15].

However, recent works about cable-driven wind tunnel mechanism (CDWTM) have focused on the design of 6 degree-of-freedom (DOF); further research is still under way to meet practical application. This article puts forward a new 3-DOF wind tunnel equipment based on cable-driven parallel mechanism, which can provide 3-DOF pure rotation for the scale model in wind tunnel. Because position analysis is one of the key complicated and important problems for the cable-driven parallel mechanism, the forward and inverse kinematics of the aforementioned mechanism is the main concern of the paper. In general, a numerical iterative scheme, such as Newton-Raphson method, can be applied to this problem. But such method not only demands an initial estimate that should be fairly close to the solution of the current configuration but also cannot guarantee the convergence to the actual solution. As is well known there are many methods that can be used to express transformation matrix in the closed-form solution

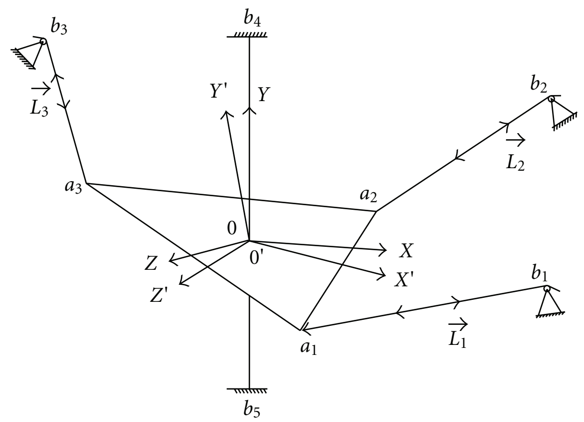

Figure 1: Functional schematic of a 3-DOF CDWTM.

for position analysis; in [16] the closed-form solution of a 3-DOF parallel manipulator is investigated by the Euler angles, resulting in a 16th degree polynomial expression in one single variable; screw theory [17, 18] is employed for the forward kinematics of the parallel mechanism; Husty [19] developed an algorithm for solving the direct kinematics of general Stewart-Gough platforms by using Euler parameters; an univariate polynomial of 40th degree is obtained; Lee and Shim et al. [20]. presented the closed-form forward kinematics of the 6-6 Stewart platform with Rodridgues' parameters; 40 sets of solutions to describe the posture of the moving platform have been determined. Our goal is to develop an algebraic algorithm to provide all the solutions of forward kinematics for the 3-DOF mechanism by means of Rodridgues' parameters, and a concise forward kinematics equation can be achieved.

The reminder of the paper is the following. Section 2 briefly outlines the system. Section 3 presents a method to obtain the analytical solution of forward kinematics. Sections 4 and 5 cover a numerical example, and conclusions are given in the last section.

2. Description of the 3-DOF CDWTM

Figure 1 shows the kinematic model of the CDWTM with the scale model, spherical joint, five cables, and the base (the wind tunnel). For convenience sake, the scale model is substituted for moving platform $a_1a_2a_3$. The spherical joint is fixed in the center of moving platform, one end of the cables Ob_4, Ob_5 is connected to the spherical joint, and the other ends b_4 and b_5 are attached to the upper and lower walls of the wind tunnel, respectively. The CDWTM can achieve 3-DOF rotational motion about point O when the other three cables $a_1b_1, a_2b_2,$ and a_3b_3 are actuated cooperatively via the motors and pulleys fixed in wind tunnel, which is very suitable for changing the three angles of the scale model in wind tunnel test. The base coordinate frame $\{OXYZ\}$ is located in spherical joint, with origin placed in the center of the spherical joint. The x-axis is against the streamline flow, the y-axis is along lift force, and the z-axis is coincident with side force. The frame $\{OX'Y'Z'\}$ is attached to the moving platform, origin is the same with the base frame. Here, vector $\mathbf{L_i}$ connects the couple vertices a_i and b_i $(i = 1, 2, 3)$. The forward kinematics of the CDWTM is to determine the orientation of the moving platform while the lengths of the three cables, $L_1, L_2,$ and L_3 are known. $\gamma, \beta,$ andα are orientation of the scale model, which is formed by rotating the axis X, the axis Y, and the axis Z, respectively.

3. Analysis of Forward Kinematics

3.1. Rodridgues' Parameter Description of the Rotational Matrix. Choose Rodridgues vector $\mathbf{u} = \{x, y, z\}^T$, and it's opposite corresponding symmetry matrix is $\mathbf{U} = \begin{bmatrix} 0 & -z & y \\ z & 0 & -x \\ -y & x & 0 \end{bmatrix}$; here $x, y,$ and z are called Rodridgues' parameters. According to Cayley's formula [21], the transformational matrix $\mathbf{R}$ can be written as follows:

$$\mathbf{R} = (\mathbf{I} - \mathbf{U})^{-1}(\mathbf{I} + \mathbf{U}). \tag{1}$$

Here $\mathbf{I}$ is a unit 3×3 matrix.

Furthermore, the inverse of $[\mathbf{I} - \mathbf{U}]$ can be represented as a function of vector $\mathbf{U}$, that is,

$$(\mathbf{I} - \mathbf{U})^{-1} = \frac{\mathbf{I} + \mathbf{U} + uu^T}{1 + u^T u}. \tag{2}$$

Taking (2) into (1), then we have

$$\mathbf{R} = \frac{(1 - \mathbf{u}^T\mathbf{u})\mathbf{I} + 2\mathbf{U} + 2\mathbf{u}\mathbf{u}^T}{1 + \mathbf{u}^T\mathbf{u}}. \tag{3}$$

3.2. Solution Procedure. From the geometric relationship in Figure 1, we can have

$$\mathbf{L}_i = \mathbf{R}\mathbf{a}_i - \mathbf{b}_i \quad (i = 1, 2, 3), \tag{4}$$

where $\mathbf{a}_i$ and $\mathbf{b}_i$ denote the position vectors a_i and b_i, respectively.

So the following equation can be obtained:

$$L_i^2 = a_i^2 + b_i^2 - 2\mathbf{b}_i^T\mathbf{R}\mathbf{a}_i \quad (i = 1, 2, 3), \tag{5}$$

where, L_i, a_i, and b_i are the norms for the corresponding vectors $\mathbf{L}_i$, $\mathbf{a}_i$, and $\mathbf{b}_i$, respectively.

For the convenience, let $\mathbf{e}_i$ and $\mathbf{f}_i$ be the unit vector for the vertices vectors $\mathbf{a}_i$ and $\mathbf{b}_i$, respectively, that is,

$$\mathbf{e}_i = \frac{\mathbf{a}_i}{a_i}, \quad \mathbf{f}_i = \frac{\mathbf{b}_i}{b_i} \quad (i = 1, 2, 3). \tag{6}$$

And also set

$$\cos\theta_i = \frac{-L_i^2 + a_i^2 + b_i^2}{2a_ib_i}, \quad \cos\theta_{0i} = \mathbf{e}_i^T\mathbf{f}_i \quad (i = 1, 2, 3). \tag{7}$$

Here, the physical meaning of θ_{0i} is the initial angle of θ_i. So (5) can be rewritten in a concise form as

$$\mathbf{f}_i^{\mathbf{T}}\mathbf{R}\mathbf{e}_i = \cos\theta_i \quad (i = 1, 2, 3). \tag{8}$$

Substitute (3) into (8), and multiply both sides by the nonzero factor $(1 + \mathbf{u}^T\mathbf{u})$. (8) becomes

$$\mathbf{u}^T\mathbf{W}_i\mathbf{u} + 2\mathbf{H}_i^T\mathbf{u} = \cos\theta_i - \cos\theta_{0i} \quad (i = 1, 2, 3), \tag{9}$$

where,

$$\mathbf{W}_i = \mathbf{f}_i\mathbf{e}_i^T + \mathbf{e}_i\mathbf{f}_i^T - (\cos\theta_i + \cos\theta_{0i})\mathbf{I}, \quad \mathbf{H}_i = \mathbf{e}_i \times \mathbf{f}_i \quad (i = 1, 2, 3). \tag{10}$$

There are three unknowns in (9), which are x, y, and z. By eliminating two of the variables, the eighth polynomial in one variable can be algebraically achieved.

In order to obtain the polynomial, we let $a_i = [a_{i1}, a_{i2}, a_{i3}]^T$ and $b_i = [b_{i1}, b_{i2}, b_{i3}]^T (i = 1, 2, 3)$; taking the initial conditions into (10), we have

$$\mathbf{W}_i = \begin{bmatrix} w_{i11} & w_{i12} & w_{i13} \\ w_{i21} & w_{i22} & w_{i23} \\ w_{i31} & w_{i32} & w_{i33} \end{bmatrix} \quad (i = 1, 2, 3),$$

$$\mathbf{H_1} = (h_1, h_2, h_3), \quad \mathbf{H_2} = (h_4, h_5, h_6), \quad \mathbf{H_3} = (h_7, h_8, h_9). \tag{11}$$

Here, $\mathbf{W}_i$ and $\mathbf{H}_i$ are known from the initial conditions and (10).

According to (11), (9) can be rewritten in the following scalar equations:

$$\begin{aligned} &w_{111}x^2 + w_{122}y^2 + w_{133}z^2 + (w_{112} + w_{121})xy \\ &\quad + (w_{113} + w_{131})xz + (w_{123} + w_{132})yz \\ &\quad + 2h_1x + 2h_2y + 2h_3z = d_1, \\ &w_{211}x^2 + w_{222}y^2 + w_{233}z^2 + (w_{212} + w_{221})xy \\ &\quad + (w_{213} + w_{231})xz + (w_{223} + w_{232})yz \\ &\quad + 2h_4x + 2h_5y + 2h_6z = d_2, \\ &w_{311}x^2 + w_{322}y^2 + w_{333}z^2 + (w_{312} + w_{321})xy \\ &\quad + (w_{313} + w_{331})xz + (w_{323} + w_{332})yz \\ &\quad + 2h_7x + 2h_8y + 2h_9z = d_3 \end{aligned} \tag{12}$$

with $d_i = \cos\theta_i - \cos\theta_{0i}, (i = 1, 2, 3)$.

To derive a univariate equation in x, simplify (12) as if x is a known constant; we have

$$y^2 = p_3 + p_2y + p_1z, \tag{13}$$

$$z^2 = p_6 + p_5y + p_4z, \tag{14}$$

$$yz = p_9 + p_8y + p_7z, \tag{15}$$

where $p_1 \sim p_9$ are all the function of x; the details can be found in the appendix.

From (15), we have

$$\begin{aligned} y^2z &= p_3z + p_2yz + p_1z^2 \\ &= p_3z + p_2(p_9 + p_8y + p_7z) + p_1(p_6 - p_5y - p_4z) \\ &= y(yz) = p_9y + p_8y^2 + p_7yz \\ &= p_9y + p_8(p_3 + p_2y + p_1z) + p_7(p_9 + p_8y + p_7z) \end{aligned} \tag{16}$$

Amplify (14) by y; we can get

$$\begin{aligned} yz^2 &= y(p_6 - p_5y - p_4z) \\ &= p_6y - p_5(p_3 + p_2y + p_1z) - p_4(p_9 + p_8y + p_7z) \\ &= z(yz) = p_9z + p_8yz + p_7z^2 \\ &= p_9z + p_8(p_9 + p_8y + p_7z) + p_7(p_6 - p_5y - p_4z). \end{aligned} \tag{17}$$

We also have (18) and (19) from (16) and (17)

$$s_{11} + s_{12}y + s_{13}z = 0, \tag{18}$$

$$s_{21} + s_{22}y + s_{23}z = 0, \tag{19}$$

where

$$\begin{aligned} s_{11} &= p_1p_6 - p_3p_8 + p_2p_9 - p_7p_9, \\ s_{12} &= p_1p_5 - p_7p_8 - p_9, \\ s_{13} &= p_3 + p_1p_4 + p_2p_7 - p_7^2 - p_1p_8, \\ s_{22} &= p_2p_5 + p_6 - p_5p_7 + p_4p_8 - p_8^2, \\ s_{23} &= p_1p_5 - p_7p_8 - p_9. \end{aligned} \tag{20}$$

Similarly, amplify (15) by z; we can get

$$\begin{aligned} s_{11}z + s_{12}yz + s_{13}z^2 = s_{11}z + s_{12}(p_9 + p_8y + p_7z) \\ + s_{13}(p_6 - p_5y - p_4z) = 0, \end{aligned} \tag{21}$$

that is,

$$s_{31} + s_{32}y + s_{33}z = 0 \tag{22}$$

with

$$\begin{aligned} s_{31} &= p_6(p_3 + p_1p_4 + p_2p_7 - p_7^2 - p_1p_8) \\ &\quad + (p_1p_5 - p_7p_8 - p_9)p_9, \\ s_{32} &= (p_5(p_3 + p_1p_4 + p_2p_7 - p_7^2 - p_1p_8) \\ &\quad + p_8(p_1p_5 - p_7p_8 - p_9)), \\ s_{33} &= (p_1p_6 - p_3p_8 + p_4(p_3 + p_1p_4 + p_2p_7 - p_7^2 - p_1p_8) \\ &\quad + p_7(p_1p_5 - p_7p_8 - p_9) + p_2p_9 - p_7p_9). \end{aligned} \tag{23}$$

Table 1: Eight sets of Rodridgues' parameters.

	x	y	z
1	−0.092662	0.0143444	0.0996125
2	0.0001063 − 0.32055i	−0.282708 − 0.268418i	0.228011 − 0.218445i
3	0.0001063 + 0.32055i	−0.282708 + 0.268418i	0.228011 + 0.218445i
4	0.011217 − 0.256745i	0.209228 − 0.145614i	0.130454 + 0.129199i
5	0.011217 + 0.256745i	0.209228 + 0.145614i	0.130454 − 0.129199i
6	0.0163316 − 0.559761i	0.029079 + 0.313876i	−0.536719 + 0.0142575i
7	0.0163316 + 0.559761i	0.029079 − 0.313876i	−0.536719 − 0.0142575i
8	0.0359946	0.091278	0.0836409

In matrix form, Equations (18)–(22) can be arranged as follows:

$$\begin{bmatrix} s_{11} & s_{12} & s_{13} \\ s_{21} & s_{22} & s_{23} \\ s_{31} & s_{32} & s_{33} \end{bmatrix} \begin{bmatrix} 1 \\ y \\ z \end{bmatrix} = \mathbf{0}. \tag{24}$$

To get the nontrivial solution of (24), the determinant of the coefficient must be zero, that is,

$$\begin{aligned} |\mathbf{A}| = {} & \left((p_1p_5 - p_7p_8 - p_9)^2\right) \\ & \times \big(p_6(p_3 + p_1p_4 + p_2p_7 - p_7^2 - p_1p_8) \\ & \quad - (p_3 + p_1p_4 + p_2p_7 - p_7^2 - p_1p_8) \\ & \quad \times (p_2p_5 + p_6 - p_5p_7 + p_4p_8 - p_8^2) \\ & \quad + (p_1p_5 - p_7p_8 - p_9)p_9 \\ & \quad - (p_5(p_3 + p_1p_4 + p_2p_7 - p_7^2 - p_1p_8) \\ & \qquad + p_8(p_1p_5 - p_7p_8 - p_9)) \\ & \quad \times (p_1p_5 - p_7p_8 - p_9) \\ & \quad \times (p_1p_6 - p_3p_8 + p_2p_9 - p_7p_9) \\ & \quad - (p_3 + p_1p_4 + p_2p_7 - p_7^2 - p_1p_8) \\ & \quad \times (p_3p_5 - p_6p_7 + p_4p_9 - p_8p_9)\big) \\ & + p_1p_6 - p_3p_8 \\ & + p_4(p_3 + p_1p_4 + p_2p_7 - p_7^2 - p_1p_8) \\ & + p_7(p_1p_5 - p_7p_8 - p_9) \\ & + (p_1p_6 - p_3p_8 \\ & \quad + p_4(p_3 + p_1p_4 + p_2p_7 - p_7^2 - p_1p_8) \\ & \quad + p_7(p_1p_5 - p_7p_8 - p_9) + p_2p_9 - p_7p_9) \\ & \times ((p_2p_5 + p_6 - p_5p_7 + p_4p_8 - p_8^2) \\ & \quad \times (p_1p_6 - p_3p_8 + p_2p_9 - p_7p_9) \\ & \quad - (p_1p_5 - p_7p_8 - p_9) \\ & \quad \times (p_3p_5 - p_6p_7 + p_4p_9 - p_8p_9)) = 0. \end{aligned} \tag{25}$$

From the appendix and (18)–(22), s_{31} is a polynomial of x^4, while s_{11}, s_{21}, s_{32}, and s_{33} are all polynomials of x^3, and s_{12}, s_{13}, s_{22}, and s_{23} are only polynomials of x^2, so (25) is an eighth polynomial in one variable.

4. Example

As an example, we consider a 3-DOF CDWTM with the following initial structural parameters, the vertices vectors of the base are $b_1 = [1.6, 1.25, 1.3]^T$, $b_2 = [1.6, 1.25, -1.3]^T$, and $b_3 = [-2, 1.25, 0]^T$, the vertices vectors of the moving platform are $a_1 = [0.571581674, 0.386554, 0.11777264]^T$, $a_2 = [0.497384168, 0.408871083, -0.27465146]^T$, and $a_3 = [-0.791685337, -0.038439224, 0.14750171]^T$. The lengths of the three cables are $L_1 = 1.789090488$, $L_2 = 1.724702626$ and $L_3 = 1.77252834$. The final eighth equation about x in the example is

$$\begin{aligned} & 1.7746 \times 10^9x^8 + 1.59847 \times 10^6x^7 + 5.61258 \times 10^8x^6 \\ & \quad + 1.4869 \times 10^7x^5 + 6.75153 \times 10^7x^4 + 2.93121 \\ & \quad \times 10^6x^3 + 2.20763 \times 10^6x^2 + 145723x - 8357.62 = 0. \end{aligned} \tag{26}$$

Solving the equation, the eight sets of Rodridgues' parameters can be achieved in Table 1.

According to (3), their eight corresponding orientations are showed in Table 2.

Next we will demonstrate the validity of the analytic forward kinematics by the numerical example of inverse kinematics. Let the initial orientations of the scale model be zero, the corresponding vertices vectors of the moving platform are $a_{10} = [0.6, 0.3, 0.2]^T$, $a_{20} = [0.6, 0.3, -0.2]^T$, and $a_{30} = [-0.8, 0.1, 0]^T$. When the moving platform has a posture of $\alpha = 10^0$, $\beta = 10^0$, and $\gamma = 5^0$, the transformation matrix expressed by means of Euler angles can be showed as following

$$\begin{aligned} \mathbf{R} &= \begin{bmatrix} c\alpha c\beta & c\alpha s\beta s\gamma - s\alpha c\gamma & c\alpha s\beta c\gamma + s\alpha s\gamma \\ s\alpha c\beta & s\alpha s\beta s\gamma + c\alpha c\gamma & s\alpha s\beta c\gamma - c\alpha s\gamma \\ -s\beta & c\beta s\gamma & c\beta c\gamma \end{bmatrix} \\ &= \begin{bmatrix} 0.969846 & -0.158083 & 0.185494 \\ 0.17101 & 0.983688 & -0.0557927 \\ -0.173648 & 0.0858317 & 0.98106 \end{bmatrix}, \end{aligned} \tag{27}$$

Table 2: The eight corresponding orientations (Unit : Degree).

	α	β	γ
1	11.1374	2.65279	−10.3294
2	19.7905 − 14.0228i	−26.5992 − 24.9282i	−7.64571 − 39.2758i
3	19.7905 + 14.0228i	−26.5992 + 24.9282i	−7.64571 + 39.2758i
4	12.3115 + 8.6638i	21.2364 − 13.6688i	4.71965 − 29.9883i
5	12.3115 − 8.6638i	21.2364 + 13.6688i	4.71965 + 29.9883i
6	−55.4203 − 0.91328i	3.87121 + 1.79706i	0.70938 − 73.4251i
7	−55.4203 + 0.91328i	3.87121 − 1.79706i	0.70938 + 73.4251i
8	10	10	5

where $c\alpha = \cos\alpha$, $s\alpha = \sin\alpha$, $c\beta = \cos\beta$, $s\beta = \sin\beta$, $c\gamma = \cos\gamma$, $s\gamma = \sin\gamma$

With the help of $\mathbf{R}$, we can calculate the corresponding vertices vectors of the moving platform in the base frame

$$a_i = \mathbf{R}a_{i0} \quad (i = 1, 2, 3). \tag{28}$$

From the above equation, we have $a_1 = [0.571581674, 0.386554, 0.11777264]^T$, $a_2 = [0.497384168, 0.408871083, -0.27465146]^T$, and $a_3 = [-0.791685337, -0.038439224, 0.14750171]^T$.

So the lengths of the three cables are the norms of vectors a_ib_i, a_2b_2, a_2b_3, that is, $L_1 = 1.789090488$, $L_2 = 1.724702626$, and $L_3 = 1.77252834$.

The inverse kinematic results are the same with the initial structural parameters of the forward kinematics, which verifies that the analysis of forward kinematics is correct.

5. Conclusion

This paper presents the kinematics analysis method of a novel 3-DOF cable-driven parallel mechanism used in wind tunnel test, and then we employ elimination method to solve the analytic forward kinematics of the mechanism by using of Rodridgues' parameters, so an eighth polynomial in one variable is derived finally. A numerical example is included to verify the effectiveness and accuracy of the developed algorithm for real-time computation and control.

Appendix

We have the following:

$$\begin{aligned} a = {} & w_{132}w_{233}w_{322} - w_{122}w_{233}w_{323} - w_{122}w_{233}w_{332} \\ & + w_{133}(-w_{223}w_{322} - w_{232}w_{322} + w_{222}(w_{323} + w_{332})) \\ & - w_{132}w_{222}w_{333} + w_{122}w_{223}w_{333} + w_{122}w_{232}w_{333} \\ & + w_{123}(w_{233}w_{322} - w_{222}w_{333}), \end{aligned}$$

$$\begin{aligned} p_1 = {} & \frac{1}{a}(2h_9(w_{133}(w_{223} + w_{232}) - (w_{123} + w_{132})w_{233}) \\ & + w_{233}(2h_3(w_{323} + w_{332}) \\ & \quad + x(-w_{123} + w_{132})(w_{312} + w_{331}) \\ & \quad +(w_{113} + w_{131})(w_{\{323\}} + w_{332})) \\ & + w_{133}(-2h_6(w_{323} + w_{332}) \\ & \quad + x((w_{223} + w_{232})(w_{313} + w_{331}) \\ & \quad\quad -(w_{213} + w_{231})(w_{323} + w_{332}))) \\ & + 2h_6(w_{123} + w_{132}) - 2h_3(w_{223} + w_{232}) \\ & + x((w_{123} + w_{132})(w_{213} + w_{231}) \\ & \quad -(w_{113} + w_{131})(w_{223} + w_{232}))w_{333}), \end{aligned}$$

$$\begin{aligned} p_2 = {} & \frac{1}{a}(2h_8(w_{133}(w_{223} + w_{232}) - (w_{123} + w_{132})w_{233} \\ & + w_{233}(2h_2(w_{323} + w_{332}) \\ & + x(-(w_{123} + w_{132})(w_{312} + w_{321})) \\ & +(w_{112} + w_{121})(w_{323} + w_{332})) \\ & \times w_{133}(-2h_5(w_{323} + w_{332}) \\ & \quad + x((w_{223} + w_{232})(w_{312} + w_{321})) \\ & \quad -(w_{212} + w_{221})(w_{323} + w_{332})) \\ & + (2h_5(w_{123} + w_{132}) - 2h_{132}(w_{223} + w_{232}) \\ & \quad + x((w_{123} + w_{132})(w_{212} + w_{221}) \\ & \quad\quad -(w_{112} + w_{121})(w_{223} + w_{232})))w_{333}), \end{aligned}$$

$$
\begin{aligned}
p_3 = \frac{1}{a}(& w_{233}(w_{123}(d_3 - x(2h_7 + xw_{311})) \\
&\quad + w_{132}(d_3 - x(2h_7 + xw_{311})) \\
&\quad -(d_1 - x(2h_1 + xw_{111}))(w_{323} + w_{332})) \\
&+ w_{133}(w_{223}(-d_3 + 2xh_7 + x^2 w_{311}) \\
&\quad + w_{232}(-d_3 + 2xh_7 + x^2 w_{311}) \\
&\quad +(d_2 - x(2h_4 + xw_{211}))(w_{323} + w_{332})) \\
&- (w_{123}(d_2 - x(2h_4 + xw_{211})) \\
&\quad + w_{132}(d_2 - x(2h_4 + xw_{211})) \\
&\quad -(d_1 - x(2h_1 + xw_{111}))(w_{223} + w_{232}))w_{333}),
\end{aligned}
$$

$$
\begin{aligned}
p_4 = \frac{1}{a}(& 2h_9((w_{123} + w_{132})w_{222} - w_{122}(w_{223} + w_{232})) \\
&+ xw_{123}w_{222}w_{313} - xw_{122}w_{223}w_{313} - xw_{122}w_{232}w_{313} \\
&- 2h_6 w_{132}w_{322} - xw_{132}w_{213}w_{322} + 2h_3 w_{223}w_{322} \\
&+ xw_{113}w_{223}w_{322} + xw_{131}w_{223}w_{322} - xw_{132}w_{231}w_{322} \\
&+ 2h_{322}w_{232}w_{322} + xw_{113}w_{232}w_{322} + xw_{131}w_{232}w_{322} \\
&+ 2h_6 w_{122}w_{323} + xw_{122}w_{213}w_{323} - 2h_3 w_{222}w_{323} \\
&- xw_{113}w_{222}w_{323} - xw_{131}w_{222}w_{323} + xw_{122}w_{231}w_{323} \\
&+ xw_{132}w_{222}w_{331} - xw_{122}w_{223}w_{331} - xw_{122}w_{232}w_{331} \\
&+ w_{123}(-(2h_6 + x(w_{213} + w_{231}))w_{322} \\
&\quad +xw_{222}(w_{313} + w_{331})) \\
&+ (2h_6 w_{122} - (2h_3 + x(w_{113} + w_{131}))w_{222} \\
&\quad +xw_{122}(w_{213} + w_{231}))w_{332}),
\end{aligned}
$$

$$
\begin{aligned}
p_5 = \frac{1}{a}(& 2h_8((w_{123} + w_{132})w_{222} - w_{122}(w_{223} + w_{232})) \\
&+ xw_{132}w_{222}w_{321} - xw_{122}w_{223}w_{312} - xw_{122}w_{232}w_{312} \\
&+ xw_{132}w_{222}w_{321} - xw_{122}w_{223}w_{321} - xw_{122}w_{232}w_{321} \\
&- 2h_5 w_{132}w_{322} - xw_{132}w_{212}w_{322} - xw_{132}w_{221}w_{322} \\
&+ 2h_2 w_{223}w_{322} + xw_{112}w_{223}w_{322} + xw_{121}w_{223}w_{322} \\
&+ 2h_2 w_{232}w_{322} + xw_{112}w_{232}w_{322} + xw_{121}w_{232}w_{322} \\
&+ w_{123}(xw_{222}(w_{312} + w_{321}) \\
&\quad -(2h_5 + x(w_{212} + w_{221}))w_{322}) \\
&+ 2h_5 w_{122}w_{323} + xw_{122}w_{212}w_{323} + xw_{122}w_{221}w_{323} \\
&- 2h_2 w_{222}w_{323} - xw_{112}w_{222}w_{323} - w_{121}w_{222}w_{323} \\
&+ (w_{122}(2h_5 x(w_{212} + w_{221})) \\
&\quad -(2h_2 + x(w_{112} + w_{121}))w_{222})w_{332}),
\end{aligned}
$$

$$
\begin{aligned}
p_6 = \frac{1}{a}(& d_3 w_{122}w_{223} - 2xh_7 w_{122}w_{223} \\
&+ d_3 w_{122}w_{232} - 2xh_7 w_{122}w_{232} - x^2 w_{122}w_{223}w_{311} \\
&- x^2 w_{122}w_{232}w_{311} - d_1 w_{223}w_{322} + 2xh_1 w_{223}w_{322} \\
&+ x^2 w_{111}w_{223}w_{322} - d_1 w_{232}w_{322} + c + x^2 w_{111}w_{232}w_{322} \\
&+ w_{123}(w_{222}(-d_3 + 2xh_7 + x^2 w_{311}) \\
&\quad +(d_2 - x(2h_4 + xw_{211}))w_{322}) \\
&+ w_{132}(w_{222}(-d_3 + 2xh_7 + x^2 w_{311}) \\
&\quad +(d_2 - x(2h_4 + xw_{211}))w_{322}) \\
&- d_2 w_{122}w_{323} + 2xh_4 w_{122}w_{323} + x^2 w_{122}w_{211}w_{323} \\
&+ d_1 w_{222}w_{323} - 2xh_1 w_{222}w_{323} - x^2 w_{111}w_{222}w_{323} \\
&- (w_{122}(d_2 - x(2h_4 + xw_{211})) \\
&\quad +(-d_1 + 2xh_1 + x^2 w_{111})w_{222})w_{332}),
\end{aligned}
$$

$$
\begin{aligned}
p_7 = \frac{1}{a}(& h_9(-2w_{133}w_{222} + 2w_{122}w_{233}) \\
&+ w_{233}(-(2h_3 + x(w_{113} + w_{131}))w_{322} \\
&\quad +xw_{122}(w_{313} + w_{331})) \\
&+ w_{133}((2h_6 + x(w_{213} + w_{231}))w_{322} \\
&\quad -xw_{222}(w_{313} + w_{331})) \\
&- (2h_6 w_{122} - (2h_3 + x(w_{113} + w_{131}))w_{222} \\
&\quad +xw_{122}(w_{213} + w_{231}))w_{333}),
\end{aligned}
$$

$$
\begin{aligned}
p_8 = \frac{1}{a}(& h_8(-2w_{133}w_{222} + 2w_{122}w_{233}) \\
&+ w_{233}(xw_{122}(w_{312} + w_{321}) \\
&\quad -(2h_2 + x(w_{112} + w_{121}))w_{322}) \\
&+ w_{133}(-xw_{222}(w_{312} + w_{321}) \\
&\quad +(2h_5 + x(w_{212} + w_{221}))w_{322}) \\
&- (w_{122}(2h_5 + x(w_{212} + w_{221})) \\
&\quad -(2h_2 + x(w_{112} + w_{121}))w_{322})w_{333}),
\end{aligned}
$$

$$p_9 = \frac{1}{a}(w_{133}(w_{222}(d_3 - x(2h_7 + xw_{311})) + (-d_2 + 2xh_4 + x^2 w_{211})w_{322}) + w_{122}(w_{233}(-d_3 + 2xh_7 + x^2 w_{311}) + (d_2 - x(2h_4 + xw_{211}))w_{333}) + (d_1 - x(2h_1 + xw_{111}))(w_{233}w_{322} - w_{222}w_{333})). \quad (A.1)$$

Acknowledgment

This work was Supported by the National Defense Pre-Research Foundation of China.

References

[1] R. Aracil, R. Saltarén, and O. Reinoso, "Parallel robots for autonomous climbing along tubular structures," *Robotics and Autonomous Systems*, vol. 42, no. 2, pp. 125–134, 2003.

[2] M. Terrier, A. Dugas, and J.-Y. Hascoët, "Qualification of parallel kinematics machines in high-speed milling on free form surfaces," *International Journal of Machine Tools and Manufacture*, vol. 44, no. 7-8, pp. 865–877, 2004.

[3] Y.-J. Li, B.-Y. Sun, J. Zhang, M. Qian, and Z.-Y. Jia, "A novel parallel piezoelectric six-axis heavy force/torque sensor," *Measurement*, vol. 42, no. 5, pp. 730–736, 2009.

[4] Y. Tian, B. Shirinzadeh, and D. Zhang, "Design and dynamics of a 3-DOF flexure-based parallel mechanism for micro/nano manipulation," *Microelectronic Engineering*, vol. 87, no. 2, pp. 230–241, 2010.

[5] J. Albus, R. Bostelman, and N. Dagalakis, "The NIST Robocrane," *Journal of Robotic Systems*, vol. 10, no. 5, pp. 709–724, 1993.

[6] R. Bostelman, A. Jaco, and R. Bunch, "Delivery of an advanced double-hull ship welding system using Robocrane," in *Proceedings of the 3rd International ICSE Symposia on Intelligent Industrial Automation and Soft Computing*, Genova, Italy, 1999.

[7] R. Dekker, A. Khajepour, and S. Behzadipour, "Design and testing of an ultra-high-speed cable robot," *International Journal of Robotics and Automation*, vol. 21, no. 1, pp. 25–34, 2006.

[8] J. K. Salisbury, *Kinematic and force analysis of articulated hands*, Ph.D. dissertation, Department of Mechanical Engineering, Stanford University, Stanford, Calif, USA, 1982.

[9] S. C. Jacobsen, J. E. Wood, D. F. Knutti, and K. B. Biggers, "The Utah-MIT dexterous hand: work in progress," *International Journal of Robotics Research*, vol. 3, no. 4, pp. 21–50, 1985.

[10] J. Albus, R. Bostelman, and N. Dagalakis, "The NIST SPIDER, a robot crane," *Journal of Research of the National Institute of Standards and Technology*, vol. 97, no. 3, pp. 373–385, 1992.

[11] K. Ning, M. Zhao, and J. Liu, "A new wire-driven three degree-of-freedom parallel manipulator," *Journal of Manufacturing Science and Engineering*, vol. 128, no. 3, pp. 816–819, 2006.

[12] A. J. Madhani, G. Niemeyer, and J. K. Salisbury Jr., "The Black Falcon: a teleoperated surgical instrument for minimally invasive surgery," in *Proceedings of the IEEE/RSJ International Conference on Intelligent Robots and Systems*, vol. 2, pp. 936–944, October 1998.

[13] N. A. Patronik, M. A. Zenati, and C. N. Riviere, "A miniature cable-driven robot for crawling on the heart," in *Proceedings of the 27th Annual International Conference of the Engineering in Medicine and Biology Society*, pp. 5771–5774, Shanghai, China, September 2005.

[14] P. Lafourcade, M. Llibre, and C. Reboulet, "Design of a parallel wire-driven manipulator for wind tunnels," in *Proceedings of the Workshop on Fundamental Issues and Future Directions for Parallel Mechanisms and Manipulators*, pp. 187–194, Quebec, Canada, 2002.

[15] Z. Yaqing, L. Qi, and L. Xiongwei, "initial test of a wire-driven parallel suspension system for low speed wind tunnels," in *Proceedings of the 12th IFToMM World Congress*, Besançon, France, June 2007.

[16] G. R. Dunlop and T. P. Jones, "Position analysis of a 3-DOF parallel manipulator," *Mechanism and Machine Theory*, vol. 32, no. 8, pp. 903–920, 1997.

[17] J. Gallardo-Alvarado, J. M. Rico-Martínez, and G. Alici, "Kinematics and singularity analyses of a 4-dof parallel manipulator using screw theory," *Mechanism and Machine Theory*, vol. 41, no. 9, pp. 1048–1061, 2006.

[18] Z. Huang, W. S. Tao, and Y. F. Fang, "Study on the kinematic characteristics of 3 DOF in-parallel actuated platform mechanisms," *Mechanism and Machine Theory*, vol. 31, no. 8, pp. 999–1007, 1996.

[19] M. L. Husty, "An algorithm for solving the direct kinematics of general Stewart-Gough platforms," *Mechanism and Machine Theory*, vol. 31, no. 4, pp. 365–379, 1996.

[20] T.-Y. Lee and J.-K. Shim, "Algebraic elimination-based real-time forward kinematics of the 6-6 Stewart platform with planar base and platform," in *Proceedings of the IEEE International Conference on Robotics and Automation (ICRA '01)*, pp. 1301–1306, Seoul, South Korea, May 2001.

[21] O. Bottema and B. Roth, *Theoretical Kinematics*, North-Holland, New York, NY, USA, 1979.